Propagation of temperature and salinity anomalies in the Nordic Seas as derived from a multi-decadal OGCM simulation

by

Frank Kauker, Rüdiger Gerdes, and Cornelia Köberle

Alfred-Wegener-Institute for Polar and Marine Research, Germany

Abstract

An experiment with a coupled sea ice-ocean model of the North Atlantic and the Arctic Ocean forced with atmospheric data from the NCEP/NCAR reanalysis is analyzed with respect to long-term variability of the sea-surface temperature and the sea-surface salinity in the Nordic Seas. Lagged linear regression is used to identify anomalies related to the *North Atlantic Oscillation*, the *Arctic Oscillation*, the sea-surface temperature in the 'storm-formation region', and the ice transport through the Fram Strait which can be traced for several years. These anomalies are not restricted to the surface, but can be found up to depths of a few hundred meters.

 e-mail: fkauker@awi-bremerhaven.de

1 Introduction

The most robust pattern of atmospheric variability in the North Atlantic on seasonal to decadal time-scales in winter is the *North Atlantic Oscillation* (NAO) *[Hurrel, 1995]*. A high NAO phase is associated with anomalous warm and humid, stronger than normal westerly winds over Europe and the southern Nordic Seas. Closely related to the NAO is the *Arctic Oscillation* (AO) *[Thompson and Wallace, 1997]* defined as the leading principal component of the wintertime (Nov.-April) seasonal means of the sea level pressure (SLP) anomaly field over the domain poleward of $20^\circ N$. Here, the leading principal component is estimated from the *NCEP/NCAR* reanalysis *[Kalnay et al., 1996]* and explains 33% of the variance.

The aim of the study is to identify propagating signals in the Nordic Seas. The NAO and AO time series are used as indices for linear regression.

Another time series used is the modelled sea-surface temperature (SST) in the area $82 - 69^\circ W$, $25 - 35^\circ N$ called 'storm-formation region' (SFR) near the southeastern coast of the USA. There, severe winter land/sea temperature contrasts fuels storm development through baroclinic instability *[Roeber, 1984]*. The modelled SST times series shows fluctuation on decadal to inter-decadal time scales. The spectrum is significantly peaked at a period of 10-12 years at the 95% level which was tested by fitting AR(1) processes to the data. The modelled SST time series resembles the SST time series in the SFR derived from ship observations *[Sutton and Allen, 1997]* for the overlapping time period 1963-1988.

The fourth index used is the time series of the modelled ice transport through the Fram Strait (ITF).

Lagged linear regression is applied to the modelled SST and the modelled sea-surface salinity (SSS) as well as to subsurface fields to detect propagating signals related to the NAO, the AO, the SFR SST, and the ITF.

2 Model description, experimental design, and data preparation

The employed ocean circulation model derives from the GFDL modular ocean model (MOM-2) *[Pacanowski, 1995]*. The model domain encloses the Atlantic north of approximately $20^\circ S$ and the Arctic Ocean. The southern boundary is closed. The model is formulated on a rotated grid with a horizontal resolution of $1^\circ \times 1^\circ$. The vertical is discretized by 19 levels whereby the level thickness increases with depth. The time step of the model is 6 hours.

A dynamic-thermodynamic sea-ice model with a viscous-plastic rheology *[Harder, 1998]* based on *Hibler's [1979]* model is coupled to the ocean model. The sea-ice model employs the same grid and time step as the ocean model.

The coupled sea ice-ocean model is forced with atmospheric surface data from the *NCEP/NCAR* reanalysis. Monthly mean data were generated for surface air temperature, dew point temperature, cloudiness, and wind speed. Wind stress was taken as daily means. The precipitation was taken as climatological monthly mean from the *ECMWF* reanalysis *[Gibson et al., 1997]*.

For all model and forcing variables used in the following analysis monthly means were generated and the long-term mean annual and semi-annual cycle were subtracted. The means of the winter months November to April were calculated and 5-years running-mean were computed. The first three years of the integration were discarded, because of the cold start. Finally, the data were detrended because it is *a priori* not possible to distinguish between a model drift and a trend in the data.

e-mail: fkauker@awi-bremerhaven.de

3 Results

3.1 Indices

The (wintertime averaged, smoothed, detrended, and renormalized) time series used for the regression are shown in Fig. 1. Table 1 lists the correlation coefficient for the four time series. The NAO and the AO are highly positive correlated (.77).

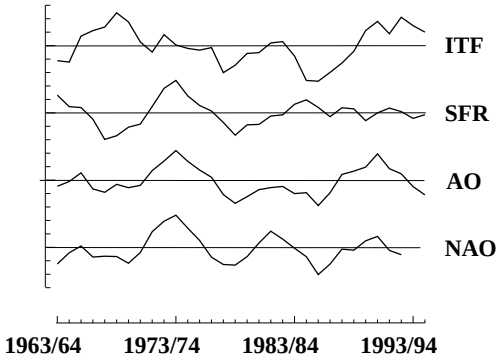

Figure 1: Comparison of Indices: (Bottom to top) Time series of the North Atlantic Oscillation (NAO), the Arctic Oscillation (AO), the SST in the 'storm-formation region' (SFR), and the ice transport through the Fram Strait (ITF) from winter 1963/64 to winter 1994/95. The time series are wintertime (Nov.-April) seasonal means, detrended, smoothed with a 5-year running mean, and renormalized to have standard deviation one.

The correlation is not constant during the integration as can be seen by comparing the correlation for winter 1963/64 to 1978/79 (Tab. 2) with winter 1979/80 to 1994/95 (Tab. 3); during the second half of the simulation the correlation is only half as high as during the first half of the simulation.

The SST in the SFR is highly positively correlated ($\approx .8$) with the NAO and the AO in the first half of the simulation but almost no correlation can be obtained during the second half.

The ice transport through the Fram Strait (ITF) is positively correlated ($\approx .6$) with the NAO and the AO in the second half. However, there is little correlation during the first half. The ITF is weakly negative correlated with the SFR time series during both time periods.

	NAO	AO	SFR	ITF
NAO		.77	.52	.31
AO			.56	.39
SFR				-.26

Table 1: Correlation statistics of the North Atlantic Oscillation (NAO), the Arctic Oscillation (AO), the SST in the 'storm-formation region' (SFR), and the ice transport through the Fram Strait (ITF) of the winters 1963/64 to 1994/95.

	NAO	AO	SFR	ITF
NAO		.93	.75	.08
AO			.84	.11
SFR				-.27

Table 2: Correlation statistics of the North Atlantic Oscillation (NAO), the Arctic Oscillation (AO), the SST in the 'storm-formation region' (SFR), and the ice transport through the Fram Strait (ITF) of the winters 1963/64 to 1978/79.

In summary, the NAO and the AO are representing almost the same information but the NAO(AO), SFR, and ITF are representing very different information.

3.2 Associated patterns

The four time series are used as indices for a lagged linear regression. To test the significance of the regression patterns AR(1) processes were fitted to the time series and the correlations were calculated. Correlations $> .4$ are significant at the 90% level, $> .5$ at the 95% level, and $> .6$ at the 99% level. Fig. 2 shows the *associated pattern* of the local SST with the NAO for time lags of one year and three years. The pattern for one year lag is shown because the correlations for one year lag are higher than for zero lag. At one year lag positive correlations on the order of $.6$ can be seen in the Barents Sea and in the Nordic Seas. Negative correlations of $\approx .7$ can be found in the Labrador Sea and east of Iceland. Amplitudes on the order of $\approx .5^{\circ}C$ are associated with the NAO in the prescripted regions of high positive and negative correlations (not shown).

Two years later the regions of high correlation in the Barents Sea and the GIN Seas have vanished but a new local region of high correlation

e-mail: fkauker@awi-bremerhaven.de

	NAO	AO	SFR	ITF
NAO		.51	-.29	.61
AO			.03	.62
SFR				-.36

Table 3: Correlation statistics of the North Atlantic Oscillation (NAO), the Arctic Oscillation (AO), the SST in the 'storm-formation region' (SFR), and the ice transport through the Fram Strait (ITF) of the winters 1979/80 to 1994/95.

can be seen in the Kara Sea. Investigation of the local heat fluxes suggest that this anomaly propagates from the Barents Sea into the Kara Sea. Amplitudes are much weaker than for one year lag (on the order of $.1°C$). The region of high negative correlations east of Iceland is shifted towards the Norwegian coast and has still amplitudes of $\approx .5°C$. Both, the anomalies in the Kara Sea and the anomalies east of Iceland can be traced for two more years with roughly the same amplitudes but lesser correlations.

Fig. 3 shows the same analysis for the AO. For one year lag the local SST in the Nordic Seas and the Barents Sea ist stronger correlated with the AO than with the NAO. Qualitatively the same propagating signals are connected with the AO and the NAO.

The associated patterns to the SST in the SFR are depicted in Fig. 4. The lag zero pattern shows correlation up to $.9$ north of Iceland and negative correlations up to .8 in the Labrador Sea. Amplitudes of $\approx .6°C$ north of Iceland and of $\approx .8°C$ in the Labrador Sea can be found. Five years later the anomaly north of Iceland is advected into the Labrador Sea. Here, the anomaly merges with a positive anomaly created in the 'storm-formation region' described by *Sutton and Allen [1997]*. It is pointed out in *Kauker et al. [1999]* that the anomaly created north of Iceland is much stronger in amplitude than the anomaly created in the SFR. The atmospheric heat flux shows no correlation with the advecting SST anomaly created north of Iceland except for lag zero. For five years lag a significant negative correlation with the heat flux is found, i.e., the ocean is heating the atmosphere.

The propagating signals are not restricted to the surface. Fig. 5 depicts the correlation of the temperature with the SST in the SFR at an almost zonal section at approximately $70°N$ (see Fig. 4 lag 5 for the location of the section). The SST anomaly north-west of Iceland is obtained up to a depth of $250\ m$. Only very small amplitudes are connected with these anomalies below the sea ice (not shown), but at the sea-ice margin and at greater depth amplitudes up to $1°C$ are reached. At the Norwegian Coast a very deep reaching signal (correlations $> .6$, amplitudes of $\approx .5°C$) can be found. We suggest that this very deep reaching signal is a combination of the signal north-west of Iceland which circulates by part in the Nordic Seas and local heat flux forcing. The very deep reaching signals are in agreement with observations of long-term variability *[Deser et al., 1996]*.

For salinity anomalies we restrict ourself to the discussion of SSS signals related to the ITF (Fig. 6). At one year lag negative SSS anomalies are associated with anomalous high ice transport through the Fram Strait (positive transport means ice transport towards the south). The anomalies are not only located close to the Fram Strait but also north of Greenland and at the southern tip of Greenland. Amplitudes of $\approx .3\ psu$ are associated with the ITF. Positive correlations up to .7 can be found in the East Siberian Sea and the Laptev Sea with amplitudes of up to $.4\ psu$. These anomalies are connected to propagating signals in the sea-ice thickness in the Arctic Ocean (cf. *Gerdes et al. [1999]*).

Three years later the area of negative correlation has shifted towards the south towards the Labrador Sea where amplitudes of $\approx .3\ psu$ are achieved. In the area of Fram Strait only locally higher correlation can be seen. The positive correlated areas in the East Siberian Sea and the Laptev sea have propagated towards the Barents Sea.

One year lagged correlations up to .7 can be found with the overturning in the Atlantic (Fig. 7). The overturning is weakened by $2\ Sv$ (not shown) five years after maximum ice transport through the Fram Strait.

4 Summary

Propagating signals of the SST and the SSS related to the NAO, the AO, SST in the 'storm-formation region', and the ice transport through

e-mail: fkauker@awi-bremerhaven.de

Fram Strait have been analyzed. It has been shown that the used indices are mutually very different (except the NAO and the AO) and therefore not surprisingly propagating signals in different areas of the Nordic Seas have been detected.

Surprisingly, not NAO(AO) related signals have the highest correlation and amplitudes in the SST and signals related to the SST in the 'storm-formation region' have highest correlation, amplitudes, and are detectable for the longest time.

The sea ice transport through the Fram Strait influences the overturning in the Atlantic. High ice export is connected with low sea-surface salinities in the Labrador Sea four years lagged and this salinity anomalies cause a reduction of the overturning.

Acknowledgments

This work was in part funded by the BMBF through grant 01 LA9823/7 and by the EC MAST III programme through grant MAS3-CT96-0070 (VEINS).

References

Deser, C., M.A. Alexander, and M.S. Timlin, Upper ocean thermal variations in the North Pacific during 1970-1991, *J. Clim., 9*, 1840-1855, 1996.

Gerdes, R., F. Kauker, C. Köberle, and M. Karcher, Possible influence of sea ice on decadal atmospheric variability over the North Atlantic? in preparation.

Gibson, J.K., P. Kallberg, S. Uppala, A. Nomura, E. Serrano and A. Hernandez, ERA description. ECMWF Reanalysis Project Report 1: Project organization. *Tech. Rep.*, European Centre of Medium Range Weather Forecast. Reading, UK, 1997.

Harder, M., P. Lemke, and M. Hilmer, Simulation of sea ice transport through Fram Strait: Natural variability and sensitivity to forcing, *J. Geophys. Res., 103(C3)*, 5595-5606, 1998.

Hibler, W.D., A dynamic thermodynamic sea ice model. *J. Geophys. Res., 9*, 815-846, 1979.

Hurrel, J.W., Decadal trends in the North Atlantic Oscillation: Regional temperatures and precipitation. *Science, 269*, 676-679, 1995.

Kalnay, E., M. Kanamitsu, R. Kistler, W. Collins, D. Deaven, L. Gandin, M. Iredell, S. Saha, G. White, J. Woollen, Y. Zhu, A. Leetmaa, R. Reynolds, M. Chelliah, W. Ebisuzaki, W. Higgins, J. Janowiak, K.C. Mo, C. Ropelewski, J. Wang, R. Jenne, and D. Joseph, The NCEP/NCAR 40-Year Reanalysis Project, *Bull. Am. Met. Soc. 77[3]*, 437-495, 1996.

Kauker, F., R. Gerdes, C. Köberle, and M. Karcher, Decadal predictability of North Atlantic sea-surface temperature as derived from a multi-decadal OGCM simulation, submitted to *Geophys. Res. Let.*, 1999.

Pacanowski, R.C., MOM 2 Documentation, user's guide and reference manual, *GFDL Ocean Group Tech. Rep. No.3*, Geophysical Fluid Dynamics Laboratory, Princeton University, Princeton, NJ.

Roeber, P.J., Statistical analysis and updated climatology of explosive cyclones. *Mon. Weath. Rev. 12*, 1577-1589, 1984.

Sutton, R.T., and M.R. Allen, Decadal predictability of North Atlantic sea surface temperature and climate, *Nature, 388*, 563-567, 1997.

Thompson, W.J., and J.M. Wallace, The Arctic Oscillation signature in the wintertime geopotential height and temperature fields, *Geophys. Res. Let., 25(9)*, 1297-1300, 1998.

e-mail: fkauker@awi-bremerhaven.de

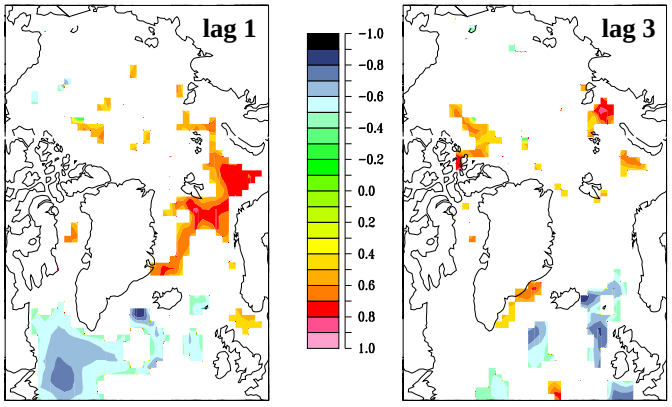

Figure 2: The fraction of low-frequency variability of local SST that can be accounted for by a linear response to the NAO. The NAO leads the local SST by the number of years drawn at each figure. Only correlations significant at the 90% level are shown.

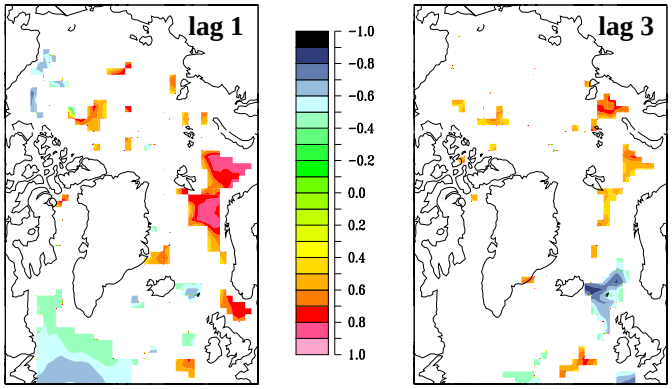

Figure 3: Same as Fig. 2 except for the AO.

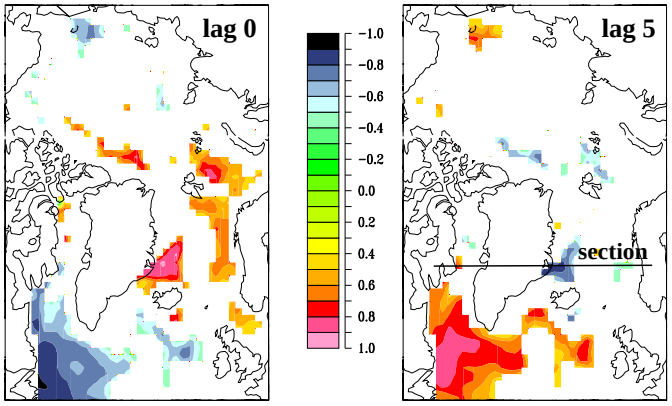

Figure 4: Same as Fig. 2 except for the SST in the SFR. The line labeled “section” indicates the position of the section shown in Fig. 5.

e-mail: fkauker@awi-bremerhaven.de

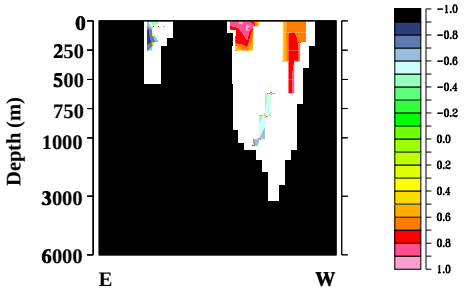

Figure 5: The fraction of low-frequency variability of the temperature on a zonal section at approximately $70^\circ N$ (cf. Fig. 4) that can be accounted for by a linear response of the SST in the SFR for zero lag. Only correlation significant at the 90% level are shown.

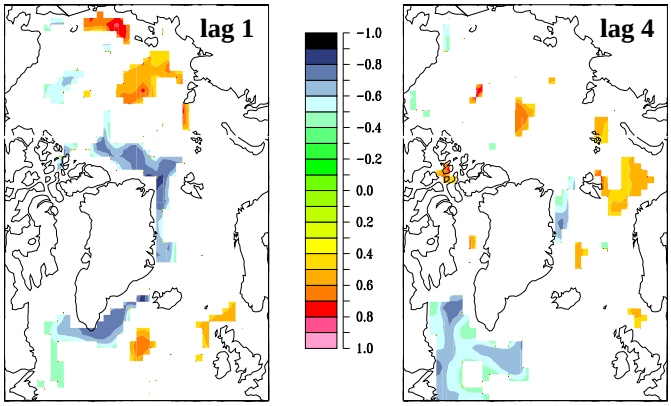

Figure 6: The fraction of low-frequency variability of local SSS that can be accounted for by a linear response to the ice transport through the Fram Strait (ITF). The ITF leads the local SSS by the number of years drawn at each figure. Only correlations significant at the 90% level are shown.

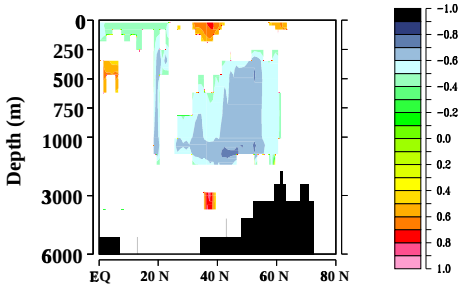

Figure 7: The fraction of low-frequency variability of the overturning that can be accounted for by a linear response of the ice transport through the Fram Strait (ITF) for five years lag. Only correlations significant at the 90% level are shown.

e-mail: fkauker@awi-bremerhaven.de